

Dispersion Compensation of the THz Communication Channels in the Atmosphere

Mahboubeh Mandehgar, and D. Grischkowsky

School of Electrical and Computer Engineering, Oklahoma State University, Stillwater, OK 74078, USA

Abstract— We demonstrate that dispersive compensation can be achieved for the communication channels within the atmospheric THz windows using the long-path THz-TDS system. However, the THz pulse broadening cannot be eliminated due to the bandwidth reduction of the propagating THz pulse due to the frequency dependent absorption of the channels.

There are many applications for relatively short-length, high bit-rate THz links in the atmosphere [1-5]. A recent study presented an experimental and theoretical characterization of short-length, high bit-rate links for the seven THz communication channels in the atmosphere below 1 THz [4]. Here, using the complete theoretical approach for the absorption and dispersion of water vapor [4-6], we show the potential to increase the bit-rate distance product, by dispersion compensation. However, we also show that the frequency dependent absorption within the channel significantly reduces the bandwidth of the transmitted signal. This reduction also broadens the THz data pulses, and consequently dispersion compensation cannot eliminate all of the observed pulse broadening with propagation. THz pulses experience distortion and broadening when they propagate through the dispersive atmosphere, which leads to overlapping of adjacent pulses in the bit sequence. Here, we analyze the increase of the performance of the Channel 7 at 852 GHz, with dispersion-compensation to demonstrate achievable high data rates of the future THz wireless network.

Dispersion management compensates phase dispersion in communication channels. Such compensation has been studied since 1980, and is used in optical fibers to significantly increase the data rates in optical communications. It is also important to understand the full capacity of the THz channels without being limited by dispersion and to be able to estimate the dispersion tolerance of the THz channels.

When the electric field of the input THz pulse, $E(0, \omega)$, (expressed as a function of frequency) passes through the dispersive atmosphere, the phase changes due to the resonance lines of water vapor. The output complex spectrum $E(z, \omega)$, is given by the product of the input field with the phase function and the attenuation, as

$$E(z, \omega) = E(0, \omega) \cdot e^{i\Delta k(\omega)z} \cdot e^{-\alpha(\omega)z/2}. \quad (1)$$

$$\Phi(\omega) = \Delta k(\omega)z = \beta(\omega)z \quad (2)$$

Here, $\beta(\omega)$ is the propagation vector, $\alpha(\omega)$ is the attenuation coefficient, $\Phi(\omega)$ is the spectral phase function and z is the propagation distance. For communication channels, $\beta(\omega)$ is approximated by a Taylor series with respect to the carrier (center) angular frequency ω_0 , as shown below

$$\beta_A(\omega) = \beta(\omega_0) + \beta_1(\Delta\omega) + \frac{1}{2}\beta_2(\Delta\omega)^2 + \frac{1}{3!}\beta_3(\Delta\omega)^3 \quad (3)$$

for Eq. (2) of [4], for which $\Delta\omega = (\omega - \omega_0)$. The term $\beta(\omega_0)$ adds a constant phase. β_1 , β_2 and β_3 are the first, second and third derivatives of $\beta(\omega)$ with respect to ω , respectively. The term, β_1 is equal to $1/v_g$, for which v_g is the group velocity, adds delay to the pulse. Neither of these terms affects the pulshape. β_2 is known as the group velocity dispersion (GVD) and is proportional to $d(1/v_g)/d\omega$. β_2 introduces a linear transit time variation with frequency for the spectral components, thereby creating temporal broadening. β_3 causes cubic phase dispersion with respect to the center frequency.

Here we provide dispersion compensation not only for the second order group delay dispersion, but also for the third-order dispersion. Higher order terms are negligible in our calculations. In order to compensate the dispersion over a large frequency range, it is helpful to rewrite the approximate phase equation $\Phi_A(\omega, z) = \beta_A(\omega)z$, in the form

$$\Phi_A = \Phi_0 + A_1 \Delta\omega + A_2 \Delta\omega^2 + A_3 \Delta\omega^3. \quad (4a)$$

$$\Phi_c = A_2 \Delta\omega^2 + A_3 \Delta\omega^3. \quad (4b)$$

The THz-bit pulse reshaping and broadening are due to the A_2 and the A_3 terms, while $\Phi_0 = \beta(\omega_0)z$ and A_1 determine the speed of undistorted pulse propagation. The compensating phase modulation is given by Φ_c . Specifying this dependence, the curve fitting tool of MATLAB was used to optimize the 3-A coefficients to fit the calculated phase Φ_A over the bandwidth.

The phase fitting is very sensitive to the water vapor resonant line structure within and near the THz communication channel under study, and the best dispersion compensation may require center frequency adjustment and bandwidth reduction. The optimal performance is obtained, when the phase fitting process to determine the A parameters is done within the output FWHM amplitude spectral range. These A parameters are then used to calculate $\Phi_A(\omega, z)$ and Φ_c over the entire spectrum. The dispersion compensation is performed by multiplying the complex output spectrum by $\exp(-i\Phi_c)$.

Our approach is equivalent to fitting the frequency dependent phase $\Phi(\omega, z)$ of the propagated pulse, due to the refractivity $(n(\omega) - 1)$, where $n(\omega)$ is the index of refraction. For our case, we remove the strong linear phase ramp as follows: $\Phi(\omega, z) = (\omega/c)(n(\omega) - n(0) - 2)z = \beta(\omega)z$, for which $(n(0) - 1) = (61.06 \times 10^{-6})$ [6].

Figure 1 shows the recently studied input THz bit sequence (011010) for the 852 GHz channel and the measured and calculated output THz bit sequence [4]. The dispersion compensated bit sequence is shown as the bottom sequence in the figure. Clearly, the transmitted bit sequence has been improved by the compensation, but the clarity of the input sequence has not been obtained.

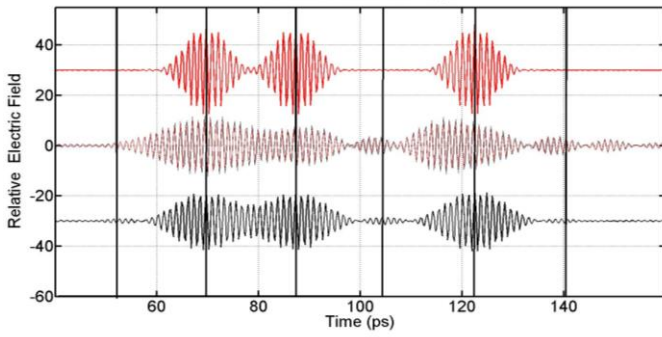


Fig. 1. Comparison of experiment and theory for **Channel 7**, 852 GHz, 56.8 Gb/s, (15 cycles), 108 GHz BW, for 137-m path propagation with RH 65% (11.2 g/m^3) and $21 \text{ }^\circ\text{C}$ [4]. The black vertical lines mark the centers of the bit slots. Upper (red) input pulses, divided by 4 for better display. Middle (red) simulated output pulses, together with overlapping middle (black) measured output pulses [4]. Lower (black) dispersion compensated IFFT output pulses.

Fig. 2 shows a single THz input pulse, the transmitted output pulse, a completely dispersion compensated output pulse, and the corresponding amplitude spectra. The output spectrum is shown with reduced amplitude due to the frequency-dependent absorption of the channel. The FWHM bandwidth of the output spectrum is 76 GHz compared to the input bandwidth of 108 GHz. This reduction in bandwidth increases the width of the completely dispersion compensated output pulse shown in Fig. 2(a), compared to the input pulse. The compensated output pulse is simply obtained by the Inverse Fast Fourier Transform (IFFT) of the output amplitude spectrum. The increased transform limited output pulsewidth is inversely proportional to the reduced bandwidth of the output spectrum.

It is a mathematical fact, that the IFFT of the amplitude spectrum of an arbitrary phase modulated pulse will give the transform limited, dispersion compensated, pulseshape. The technical question is whether this can be achieved with physically realizable linear filters or phase modulators.

Figure 3 compares the IFFT compensated pulse with the (A_2 and A_3), dispersion compensated pulse, which shows excellent compensation.

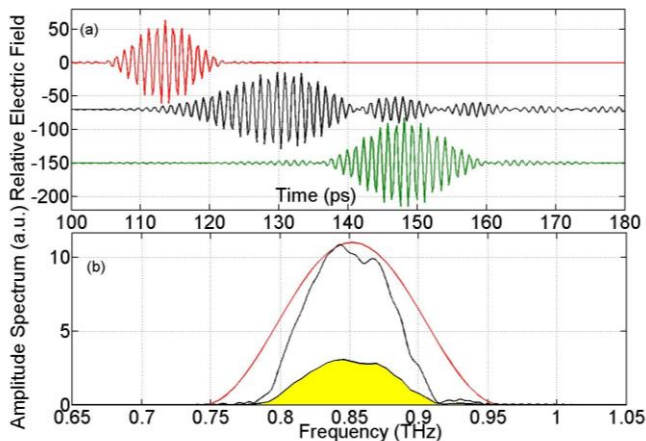


Fig. 2. (a). Upper (red) input pulse, middle (black) transmitted output pulse and lower (green) IFFT dispersion compensated output pulse, both multiplied by 3.5. Pulses are shown from 100 to 180 ps. (b). Input amplitude spectrum upper (red) line and output amplitude spectrum lowest (black) high-lighted line, also shown with multiplication as the middle (black) line.

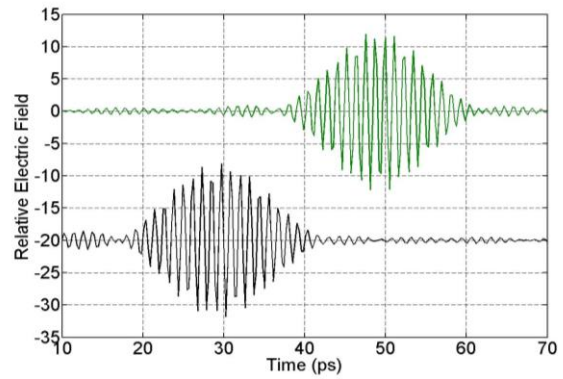


Fig. 3. Upper (green) IFFT dispersion compensated output pulse. Lower (black) output pulse with (A_2 and A_3), dispersion compensation.

Figure 4a shows the complete phase calculation of $\beta(\omega)z$ without the constant (zero frequency) refractivity term [3-6], compared to the 3-A parameter fit of Φ_A , with $(\omega_o/2\pi) = 852 \text{ GHz}$, marked by the vertical line. The difference between the two plots (residuals) is shown in Fig. 4b, indicating a good, fitting precision of the order of 0.05 rad. Figure 4c shows the compensating phase modulation Φ_c , which could be applied to the local oscillator for phase compensated, coherent detection.

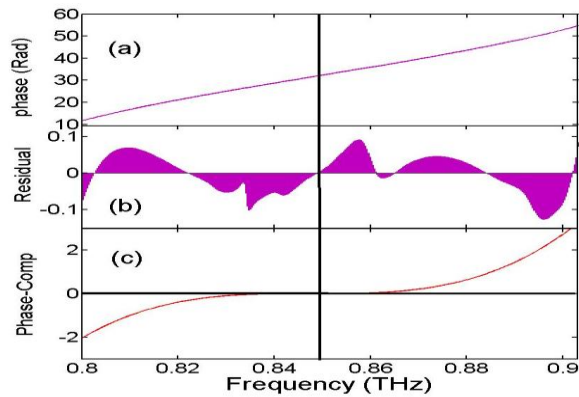


Fig. 4. All curves are shown in radians. (a). Calculated phase angle Φ for the conditions of Fig. 1 [2] (black line) and the 3-A parameter Φ_A result of Eq. (2a) (purple line). (b). Residual plot between the two (a) curves. (c). Compensating phase modulation Φ_c .

- [1]. J. Wells, "Faster than Fiber: The Future of Multi-Gb/s Wireless," IEEE Microwave Magazine, May 2009, 104–112.
- [2]. Ho-Jin Song and Tadao Nagatsuma, "Present and Future of Terahertz Communications," IEEE Trans. THz Sci. Technol. 1(1), 256–263 (2011).
- [3]. M. Mandehgar, Y. Yang and D. Grischkowsky, "Atmosphere characterization for simulation of the two optimal wireless terahertz digital communication links," Opt. Lett. Vol. 38, pp. 3437-3440, (2013).
- [4]. M. Mandehgar, Y. Yang and D. Grischkowsky, "Experimental confirmation and physical understanding of ultra-high bit rate impulse radio in the THz digital communication channels of the atmosphere," Institute of Physics, Journal of Optics, Vol. 16, 094004 (17 pp) (2014).
- [5]. Y. Yang, M. Mandehgar and D. Grischkowsky, "THz-TDS Characterization of the Digital Communication Channels of the Atmosphere," J. Infrared Milli Terahz Waves, Vol. 36, pp. 97-129 (2015) doi:10.1007/s10762-014-0099-3.
- [6]. D. Grischkowsky, Yihong Yang, and Mahboubeh Mandehgar, "Zero-Frequency Refractivity of Water Vapor, Comparison of Debye and van-Vleck Weisskopf Theory," Optics Express, Vol. 21, pp. 18899-18908 (2013).